Journal of Physiology (1993), **465**, *pp.* 223–244
With 10 figures
Printed in Great Britain

KINETIC PROPERTIES OF NMDA RECEPTOR-MEDIATED SYNAPTIC CURRENTS IN RAT HIPPOCAMPAL PYRAMIDAL CELLS *VERSUS* INTERNEURONES

BY MICHAEL PEROUANSKY* AND YOEL YAARI

From the Department of Physiology, Hebrew University School of Medicine, Jerusalem, Israel

(*Received 30 July 1992*)

SUMMARY

1. Whole-cell tight-seal recordings were obtained from visually identified pyramidal cells (PCs) and interneurones (INs) in the CA1 field of thin hippocampal slices from 13- to 23-day-old rats. The INs sampled were classified according to their location either in the molecular layer (M-INs) or in the oriens layer and alveus (OA-INs). PCs and INs differed in their mode of firing when depolarized by a prolonged current pulse. Whereas PCs fired a single action potential, most INs responded with non-accommodating high frequency spike firing.

2. In the presence of 1 μM tetrodotoxin (TTX), bath application of either 50 μM L-glutamate with 10 μM 6-cyano-7-nitroquinoxaline-2,3-dione (CNQX) or 2·5 μM *N*-methyl-D-aspartate (NMDA), induced a similar conductance increase in PCs and INs that was completely blocked by 200 μM DL-2-amino-5-phosphonovaleric acid (APV). The NMDA receptor-mediated currents reversed around 4 mV and exhibited an area of negative slope conductance at potentials more negative than -20 to -30 mV in the presence of 1–2 mM Mg^{2+}.

3. Dual-component excitatory postsynaptic currents (EPSCs) were evoked in PCs and INs by stimulating afferent fibres close to the neurone. The NMDA receptor-mediated component of the EPSCs (NMDA EPSC) was isolated by adding 10 μM CNQX to block non-NMDA receptors. The NMDA EPSCs in all cell types reversed around 1·5 mV and were abolished by 50 μM APV.

4. In saline containing 1 mM Mg^{2+}, the peak current–voltage (*I–V*) relationship of NMDA EPSCs in PCs and INs showed an area of negative slope conductance at voltages more negative than -20 to -30 mV. In nominally Mg^{2+}-free saline, the peak *I–V* relation was linear over a much wider voltage range in both cell types.

5. The 10–90% rise times of NMDA EPSCs at -60 mV ranged from 4·5 to 16 ms in PCs (mean 8·7 ms; $n = 25$) and in M-INs (mean 9·1 ms; $n = 10$). Their decay could be best fitted with the sum of two exponentials. The decay of NMDA EPSCs in PCs was significantly slower than that recorded in INs. The average fast (τ_f) and slow (τ_s) time constants of decay were, respectively, 66·5 and 353·9 ms in PCs, and 34·4 and 212·5 ms in M-INs. The corresponding mean fast (A_f) and slow (A_s) current

* Present address: Department of Anesthesiology, Hadassah Hospital, POB 12000, Jerusalem 91120, Israel.

MS 1658

amplitude components of the NMDA EPSCs were −96·8 and −86·8 pA in PCs, and −43 and −96·8 pA in M-INs.

6. The time course of NMDA EPSCs in OA-INs ($n = 37$) was considerably more variable. In 18·9% of the cells the rise times were in the ordinary range (4·5–10 ms; mean 6·9 ms) and the decay was biexponential (mean τ_f and τ_s, 49 and 212 ms; mean A_f and A_s, −76·3 and −137·2 pA, respectively). In 73% of OA-INs the rise times were very slow (18–53 ms; mean 31·2 ms) and decayed monoexponentially (mean time constant 217·2 ms). The remaining 8% had rise times in the ordinary range (10–14 ms; mean 11·7 ms) but decayed as a single exponential (mean time constant 226 ms).

7. Changes in holding voltage had no systematic effect on rise time and decay of ordinary and slow NMDA EPSCs.

8. Neither changing the site of stimulation, nor modulating the amount of glutamate release by varying stimulus intensity, lowering extracellular Ca^{2+} or adding Cd^{2+} to the saline, affected the rise time or the decay of slow NMDA EPSCs.

9. We conclude that PCs and INs in area CA1 of the rat hippocampus express NMDA EPSCs with different kinetic characteristics. NMDA EPSCs in the majority of OA-INs display unusually slow rise times.

INTRODUCTION

In the mammalian central nervous system, rapid excitatory neurotransmission is achieved primarily by glutamate acting on non-*N*-methyl-D-aspartate (NMDA) receptor-gated ion channels. In many neurones, however, the excitatory postsynaptic current (EPSC) contains also a slow component, mediated by the Ca^{2+}-permeable NMDA subtype of glutamate receptor-gated channels (NMDA EPSC). This component can be isolated pharmacologically with glutamate antagonists selective for the non-NMDA receptors (Andreasen, Lambert & Jensen, 1989). It is blocked by extracellular Mg^{2+} at negative holding potentials (Nowak, Bregestowski, Ascher, Herbet & Prochiantz, 1984; Mayer, Westbrook & Guthrie, 1984) but increases as the neurone depolarizes. Because of this distinctive voltage sensitivity, which endows synaptic transmission with regenerative properties, and the coupling of NMDA receptor activation to postsynaptic Ca^{2+} influx (MacDermott, Mayer, Westbrook, Smith & Barker, 1986) and second messenger cascades (Smart, 1989), NMDA EPSCs are thought to contribute to various forms of synaptic plasticity, such as the induction of long-term potentiation (Harris, Ganong & Cotman, 1984; Collingridge, Herron & Lester, 1988) and kindling of epileptic seizures (McNamara, Russel, Rigsbee & Bonhaus, 1988; Mody, Stanton & Heinemann, 1988).

Recent studies employing high resolution whole-cell patch-clamp recordings from visually identified neurones in thin brain slices (Edwards, Konnerth, Sakmann & Takahashi, 1989) have hinted at possible physiological variations of NMDA EPSCs. Whereas the decay of NMDA EPSCs in dentate granule cells markedly increased with depolarization (Konnerth, Keller, Ballanyi & Yaari, 1990; Keller, Konnerth & Yaari, 1991), the decay of NMDA EPSCs in CA1 pyramidal cells (PCs) was voltage insensitive (Hestrin, Nicoll, Perkel & Sah, 1990*a*). Since the NMDA EPSC decay is determined primarily by channel kinetics (Hestrin, Sah & Nicoll, 1990*b*), these

findings suggest a heterogenous expression of NMDA receptor channels in different cell types or in different brain regions.

The CA1 field of the hippocampus contains the highest density of NMDA receptors in the rat brain (Monaghan & Cotman, 1985). To further characterize the functional diversity of NMDA EPSCs, we compared these currents in different types of CA1 neurones, namely PCs and interneurones (INs) in the molecular (M-INs) and in the oriens layer and alveus (OA-INs). Significant differences in NMDA EPSC kinetics between and within cell groups were found.

METHODS

Preparation of slices

Experiments were performed on thin hippocampal slices from 13- to 23-day-old rats. Methods for preparation of thin hippocampal slices were similar to those described elsewhere (Edwards *et al.* 1989). Briefly, rats were anaesthetized with ether and decapitated with a guillotine. The brain was quickly removed and cooled in ice-cold standard saline. A block of tissue containing one hippocampus was glued with cyanoacrylate to the stage of a vibratome with its longitudinal axis vertical to the blade and bathed in cold saline.

Transverse slices of 150 μm thickness were cut from the hemispheral region containing the anterior hippocampus to preserve as much as possible the fibre system running parallel to the cutting plane. The hippocampal part was dissected out of each slice and transferred to an incubation chamber containing oxygenated standard saline at 34 °C. Slices were used one at a time after at least 1 h of incubation. In the recording chamber the slice was continuously perfused (2·5 ml min^{-1}) with oxygenated saline at room temperature (19–22 °C).

Solutions and drugs

The standard saline used for dissection and maintenance of slices consisted of (mM): NaCl, 125; KCl, 2·5; $NaHCO_3$, 31; Hepes, 13; NaH_2PO_4, 1·25; glucose, 12·5; $CaCl_2$, 1·5; and $MgSO_4$, 2; pH 7·3. All experimental salines in addition contained bicuculline methiodide (10 μM) to block GABA-mediated chloride currents, 6-cyano-7-nitroquinoxaline-2,3-dione (CNQX, 10 μM) to block non-NMDA receptors (Blake, Brown & Collingridge, 1988; Honore, Davies, Drejer, Fletcher, Jacobsen, Lodge & Nielsen, 1988) and glycine (10 μM) to ensure saturation of the glycine binding sites of NMDA receptors (Thomson, Walker & Flynn, 1989) and to increase the selectivity of CNQX to the non-NMDA receptors (Birch, Grossmann & Hayes, 1988). The concentration of Ca^{2+} was increased to 2·5 mM, whereas Mg^{2+} was either omitted completely or added at the specified concentrations. Saline without added Mg^{2+} is referred to as Mg^{2+} free. In one series of experiments either L-glutamate (20–50 μM) with CNQX (10 μM) or *N*-methyl-D-aspartate (2·5–5 μM) were applied via bath perfusion together with tetrodotoxin (TTX, 1 μM) to block neurally evoked transmitter release. The resulting current in voltage-clamped cells reached a steady state within about 30 s, after a delay caused by exchange of solution in the dead space of the perfusion system.

The intracellular (pipette) solution in voltage-clamp experiments consisted of (mM): CsF, 130/NaCl, 10; Hepes, 10; EGTA, 10; $MgCl_2$, 2; $CaCl_2$, 1. In current-clamp experiments, CsF was replaced by KF (130 mM). The pH was adjusted to 7·2–7·3. The osmolarity was close to the measured osmolarity of the extracellular solution (300–310 mosmol). Fluoride was used to reduce voltage-dependent Ca^{2+} currents (Kostyuk, Krishtal & Pidoplichko, 1975; Kay, Miles & Wong, 1986), thus improving space clamp. In our hands it virtually abolished high threshold-activated Ca^{2+} currents within 10–15 min after establishing the whole-cell configuration. Cs^+ reduced potassium conductances. In some experiments 2(triethylamino)-*N*-(2,6-dimethylphenyl)acetamide (QX-314; 20–50 μM) was added to the pipette solution to suppress Na^+-mediated spikes (Frazier, Narahashi & Yamada, 1970; Connors & Prince, 1982).

Drugs were purchased from Sigma Chemical Co., with the exception of 6-cyano-7-nitroquinoxaline-2,3-dione (CNQX, Tocris Neuramin, England) and QX-314 (courtesy of Astra Pain Control AB, Sweden).

Experimental procedure

Experiments were performed at room temperature (19–24 °C). Cells were visualised at 400× magnification with Nomarski optics using an upright Zeiss Standard 14 microscope. PCs were identified by their position within the pyramidal layer, the pyramidal shape of their somata and the prominent apical dendrite. INs were located well off the pyramidal layer either in the stratum oriens, close to the border of the alveus (OA-INs), or in the stratum radiatum/moleculare (M-INs). Their shape was non-pyramidal and they lacked a prominent apical dendrite. No attempts were made to record from INs located in, or very close to, the pyramidal layer, thus presumably excluding basket cells from our sample (Lorente de Nó, 1934).

Recording pipettes were pulled from borosilicate glass (Hilgenberg, FRG) on a vertical puller (List-medical, FRG) and coated with Sylgard resin (Dow Corning Chemical Co., USA). The series resistance (after establishment of the whole-cell mode) of about 5 MΩ was compensated for by setting the series resistance compensation control of the amplifier (List LM-EPC 7) to 50–75%. At the end of a recording session the pipette was withdrawn from the cell and the tip potential was measured and subtracted from the nominal holding potential.

The cleaning/stimulating pipettes were pulled from 'Boralex' disposable micropipettes (Rochester Scientific, USA) to a tip diameter of 6–10 μm, fire-polished to reduce damage to the tissue during stimulation, and filled with saline. The EPSCs were evoked by stimulating close (20–70 μm) to the patched cell at a frequency of 0·05 Hz, using a bipolar electrode consisting of the aforementioned cleaning pipette and a remote, 100 μm thick platinum wire connected to an isolated unit (WPI, USA). The same pipette was used for cleaning the surface of cells to be investigated to improve seal formation, following the general techniques described by Edwards *et al.* (1989).

The current–voltage (*I–V*) relationships of exogenous L-glutamate- and NMDA-induced currents were obtained by applying voltage ramps as follows: from the initial holding potential (−60 mV) the membrane potential was first stepped to +60 mV for 1020 ms to inactivate voltage-gated conductances. The voltage was changed linearly to −90 mV within 950 ms, and stepped back to −60 mV. Leak and other residual currents were eliminated from the response by subtraction of appropriate control responses obtained in the absence of agonist. The *I–V* relations of the L-glutamate- or NMDA-induced currents represent averages of six ramps in two separate applications after subtraction of control ramps.

Data analysis

All currents recorded were filtered at 3 kHz, digitized on-line at sampling rates between 0·7 and 2 kHz and analysed off-line using an Olivetti personal computer and software from Axon Instruments. Kinetic analysis was performed on averaged EPSCs (usually 5–10 consecutive traces). The rise times of NMDA EPSCs were measured at the 10–90% peak. Their decays were fitted with the exponential functions: $y = A_f e^{-t/\tau_f} + A_s e^{-t/\tau_s}$ for double and $y = A_1 \exp^{-t/\tau}$ for single exponential decay, where A is the current amplitude, τ is the decay time constant, and the subscripts f and s denote fast and slow component. The algorithms used for fitting these functions to data points minimized the least squares error between data points and calculated fit points by multiple least squares regression for amplitudes and a simplex minimization for time constants.

Measurements are given as means ± S.D. The among-group differences were tested using one-way analysis of variance (ANOVA). When significant differences were indicated in the F ratio in Snedecor's test ($P < 0{\cdot}001$), the significance of differences between means of any two of these groups was determined using the modified Tukey method for multiple comparisons with an α of 0·05.

Fitting I–V relations of NMDA conductance

The negative slope conductance in the *I–V* relation of NMDA receptor-mediated currents in the presence of extracellular Mg^{2+} is compatible with a scheme of open channel block, in which Mg^{2+} ions block the NMDA receptor channel at a site located within the electric field of the membrane (Ascher & Nowak, 1988). Assuming a one-to-one stoichiometry for the binding of extracellular Mg^{2+} ions to open NMDA receptor channels, R, the kinetic equation is:

$$Mg^{2+} + R \rightleftharpoons Mg^{2+}R$$

The dissociation constant, K_D, for this binding reaction is given by eqn (1) in which [R] and [Mg^{2+}R] are the concentrations of free and Mg^{2+}-bound open NMDA receptor channels, respectively:

$$K_D = \frac{[Mg^{2+}][R]}{[Mg^{2+}R]}. \quad (1)$$

At equilibrium, the fraction of unbound (i.e. unblocked) NMDA receptor channels, y is given by the following relation:

$$y = \frac{[R]}{[R]+[Mg^{2+}R]},$$

which can be rewritten as eqn (2):

$$y = \frac{1}{1+[Mg^{2+}]/K_D}. \quad (2)$$

Ascher & Nowak (1988) have calculated the K_D for Mg^{2+} binding from NMDA-induced single channel currents in outside-out patches from cultured mouse neurones. They found that K_D increases exponentially with membrane voltage, V, i.e.,

$$K_D = ae^{bV}, \quad (3)$$

in which a and b are constant parameters. Assuming that the K_D for Mg^{2+} binding at synaptic NMDA receptor channels is similarly an exponential function of V, and that V has no effect on the total number of NMDA receptor channels opened by the transmitter, then the fraction of unblocked open NMDA receptor channels can be expressed as a function of voltage:

$$y = \frac{a}{a+[Mg^{2+}]e^{-bV}}. \quad (4)$$

Clearly, the fraction of unblocked open NMDA receptor channels is 1, either when [Mg^{2+}] equals zero, or when V is very positive.

The conductance, g, of NMDA EPSCs is given by the relation

$$g = yg_{max},$$

in which g_{max} is the maximal conductance attained when $y = 1$. g_{max} can be measured from the linear portion of the I–V relation (at positive voltage). Therefore, g can be expressed as eqn (5):

$$g = \frac{ag_{max}}{a+[Mg^{2+}]e^{-bV}}. \quad (5)$$

The peak current during an NMDA EPSC, I is determined by g and by the driving force, according to relation (6):

$$I = g(V-V_r) \quad (6)$$

in which V_r is the reversal potential of I, which can be assessed from the experimental I–V relation.

Incorporating eqn (5) into (6), I can be expressed as a function of V and [Mg^{2+}]:

$$I = \frac{ag_{max}(V-V_r)}{a+[Mg^{2+}]e^{-bV}}. \quad (7)$$

Equation (7) describes the theoretical I–V relation of NMDA EPSCs. If [Mg^{2+}] is assumed to be the Mg^{2+} concentration in the saline, then only the values of a and b remain unknown.

RESULTS

Firing patterns

Depolarizing current was injected stepwise (10–80 pA) into six PCs and six INs (5 OA-INs; 1 M-IN) perfused internally with KF-containing pipette solution, while holding the cells at potentials close to resting membrane potential (−60 to −75 mV).

Figure 1 illustrates the distinctive responses of a PC and an OA-IN. Whereas the PC fired maximally one action potential, the IN generated a non-decrementing train of spikes at 58 Hz. Analogous responses were seen in a total of four INs and four PCs. Firing frequencies of INs ranged from 27 to 60 Hz (average 48·3 Hz). Two OA-INs

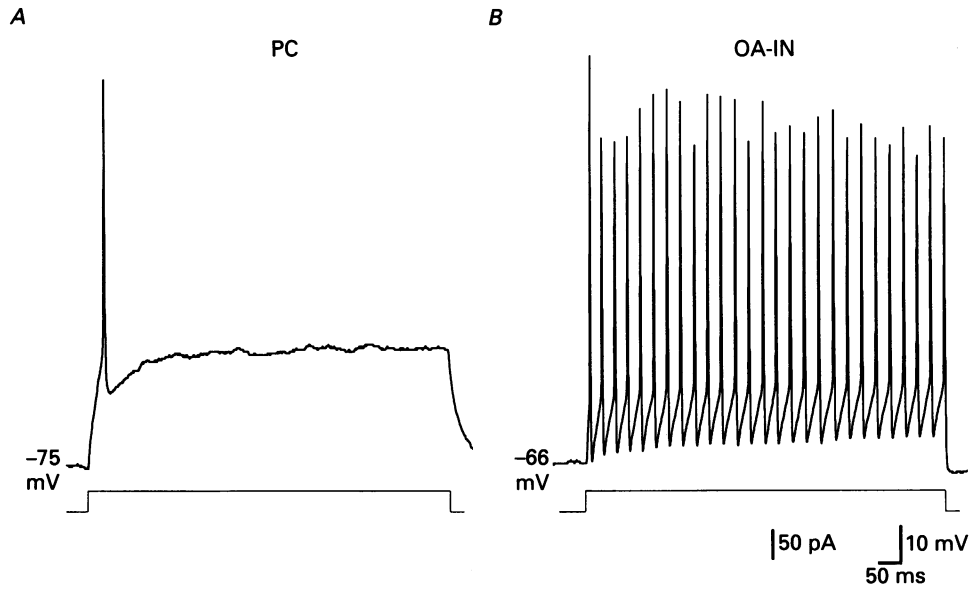

Fig. 1. Firing patterns of different CA1 neurones during maintained depolarization. A PC (*A*) and an OA-IN (*B*) were injected with 480 ms long depolarizing current pulses. Whereas the PC fired only one action potential, the OA-IN responded with repetitive firing to suprathreshold stimuli.

fired just a single spike, while two PCs fired repetitively but at much lower frequencies (16 and 18 Hz). These findings are in agreement with the evoked firing patterns of CA1 INs recorded from adult slices with conventional intracellular microelectrodes (Lacaille, Muller, Kunkel & Schwartzkroin, 1987; Lacaille & Schwartzkroin, 1988). Adult CA1 PCs, however, ordinarily generate repetitive firing which accommodates during maintained depolarization (Madison & Nicoll, 1984).

Responses to exogenous glutamate receptor agonists

Bath application of either 50 μM L-glutamate with 10 μM CNQX or 2·5 μM NMDA (with 1 μM TTX in either case) induced a conductance increase in all cells tested (seven PCs, six M-INs, nine OA-INs). The associated currents were abolished by 200 μM of the NMDA receptor blocker DL-2-amino-5-phosphonovaleric acid (APV) and blocked in a voltage-dependent manner by Mg^{2+}. These properties identified them as NMDA receptor-mediated currents. We investigated their *I–V* relation by passing voltage ramps during the steady state of the current (see Methods). Illustrative examples are shown in Fig. 2. In the three cell types the *I–V* relation in nominally 0 Mg^{2+} saline was linear down to approximately -60 mV, whereas in the

presence of Mg^{2+} an area of negative slope conductance appeared at voltages negative to −20 mV. The currents reversed at 3·5 ± 1·5 mV in PCs, 5·4 ± 2·5 mV in M-INs and 4·5 ± 1·4 mV in OA-INs. The maximal slope conductance of the response to 50 μM L-glutamate (determined at positive voltages) averaged 25·6 ± 13·9 nS in PCs, 12·2 ± 2·7 nS in M-INs and 22·9 ± 5·4 nS in OA-INs. The L-glutamate-induced conductance was significantly larger in OA-INs than in M-INs.

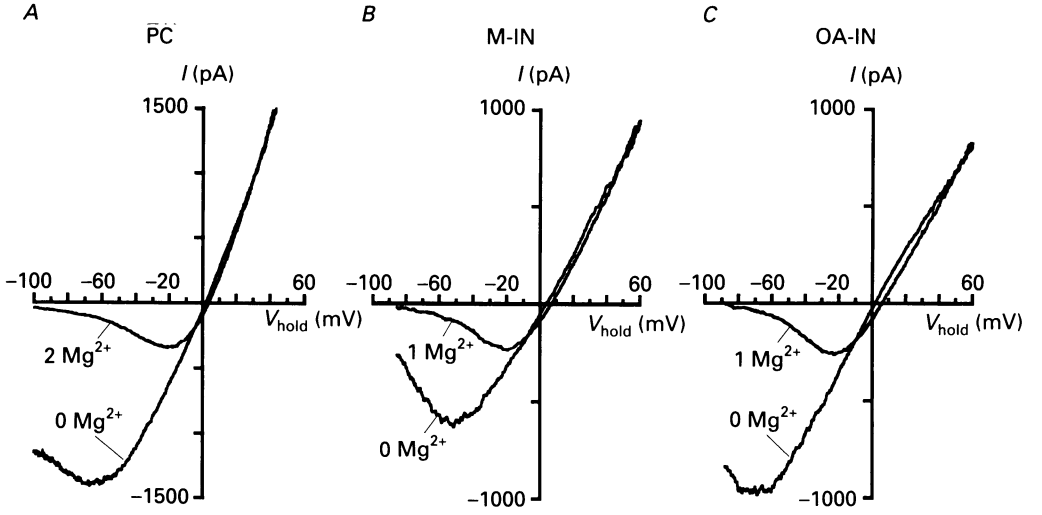

Fig. 2. *I–V* relations of agonist-induced NMDA conductances in different CA1 neurones. The PC (*A*) was perfused with saline containing 50 μM L-glutamate (with CNQX 10 μM, TTX 1 μM). The M-IN (*B*) and the OA-IN (*C*) were exposed to saline containing 2·5 μM NMDA (with TTX 1 μM). In each neurone the conductance response was first obtained in saline containing Mg^{2+} and then in nominally 0 Mg^{2+} saline. During the steady state of the conductance response, the holding current was changed linearly across the indicated voltage range. Each trace is the average of six voltage ramps after subtraction of control ramps applied in the absence of agonist to eliminate leakage currents.

Current–voltage relation of NMDA EPSCs

As recently shown in this preparation, stimulating afferent fibres in the stratum radiatum of CA1 evokes dual-component EPSCs in PCs and INs (Hestrin *et al.* 1990*a*; Sah, Hestrin & Nicoll, 1990). The fast component (rise time 1–2 ms) is mediated by non-NMDA receptors. Blockage of these receptors with micromolar concentrations of CNQX, isolates the NMDA EPSCs. All the following records referred to as NMDA EPSCs, have been obtained from CA1 PCs and INs in the presence of 10 μM CNQX. They could be blocked entirely by 50 μM APV.

Figure 3 illustrates NMDA EPSCs recorded in 1 mM Mg^{2+} saline from three representative neurones. The peak *I–V* relations of these NMDA EPSCs, with and without addition of extracellular Mg^{2+}, are shown below the sample records. The currents reversed at 0 to +3 mV (PCs: 1·6 ± 1·7 mV, $n = 10$; M-INs: 0·5 ± 0·5 mV, $n = 7$; OA-INs: 2·6 ± 1·9 mV, $n = 9$). It is evident from Fig. 2 that the *I–V* relations

of NMDA EPSCs in PCs, M-INs and OA-INs in 1 mM Mg^{2+} saline were very similar, displaying an area of negative slope conductance at voltages more negative than −20 to −30 mV. The maximal slope conductance (g_{max}) of NMDA EPSCs, derived from the *I–V* relations at positive holding potentials, averaged 3·4 ± 1·1 nS (n = 10)

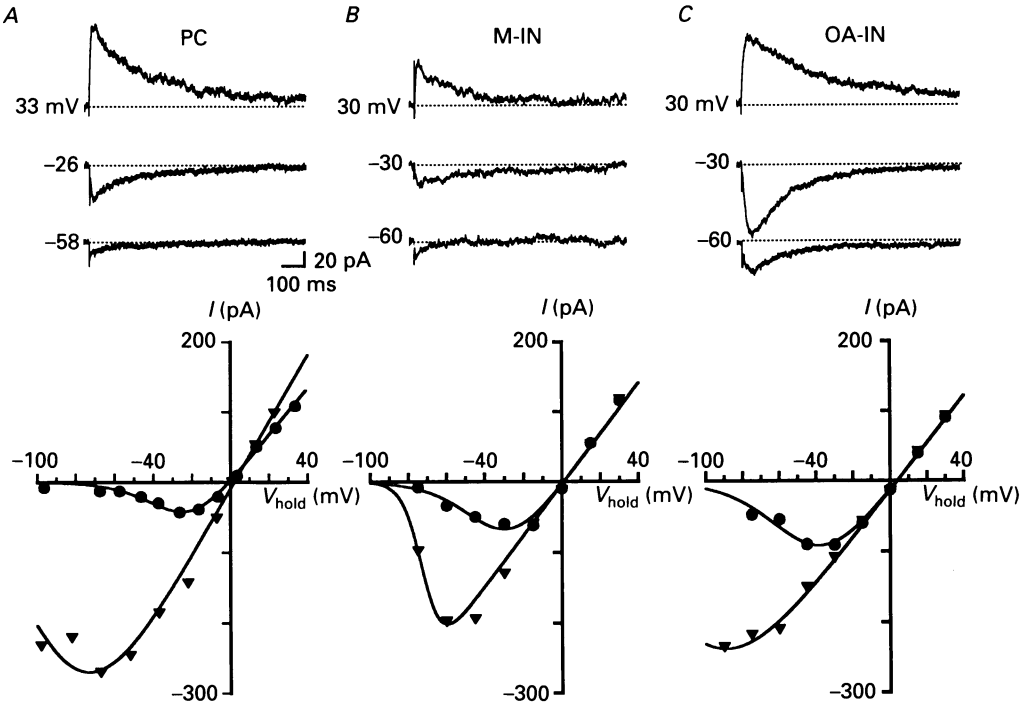

Fig. 3. Pharmacologically isolated NMDA EPSCs evoked in different CA1 neurones at different membrane potentials. The top traces illustrate NMDA EPSCs recorded at the indicated membrane potentials from a PC (*A*), a M-IN (*B*) and an OA-IN (*C*). Each trace is an average of five consecutive records. The slices were perfused with saline containing 10 μM CNQX and 1 mM Mg^{2+}. The corresponding *I–V* relations for the peak NMDA EPSCs are depicted below the traces. The circles denote the relation obtained in 1 mM Mg^{2+}. The triangles denote the relation obtained after the preparation was washed with nominally 0 Mg^{2+}. The lines through the points of the *I–V* curves were fitted with the function $I = g_{max}(V - V_r)/(1 + a[\mathrm{Mg}]e^{-bV})$ (see Methods). The values for g_{max}, as determined at positive voltages, were 3·3, 1·8, and 3·4 nS for PC, M-IN and OA-IN, respectively. The corresponding values for V_r were −0·3, 1·0 and 3·9 mV.

in PCs, 3·1 ± 2·4 nS (n = 7) in M-INs and 5·3 ± 2·7 (n = 12) in OA-INs. Washing with nominally 0 Mg^{2+} saline caused the area of negative slope conductance to shift to more negative potentials in all neurones, while only slightly, if at all, increasing g_{max}.

Rise times of NMDA EPSCs

The time course of NMDA EPSCs in the three classes of neurones was investigated in Mg^{2+}-free saline. Exemplary NMDA EPSCs are shown in Fig. 4*A*. It is clear that the rise time of the synaptic current in the OA-IN is much slower than in the other

two cells. As shown in the rise time histograms in Fig. 4*B*, the rise times of NMDA EPSCs in PCs and M-INs at holding potentials of −60 to −70 mV ranged from 4·5 to 16 ms (PCs: mean 8·7±2·5 ms, $n = 25$; M-INs: mean 9·1±3·2 ms, $n = 11$). By contrast, NMDA EPSC rise times in OA-INs showed a remarkable variability

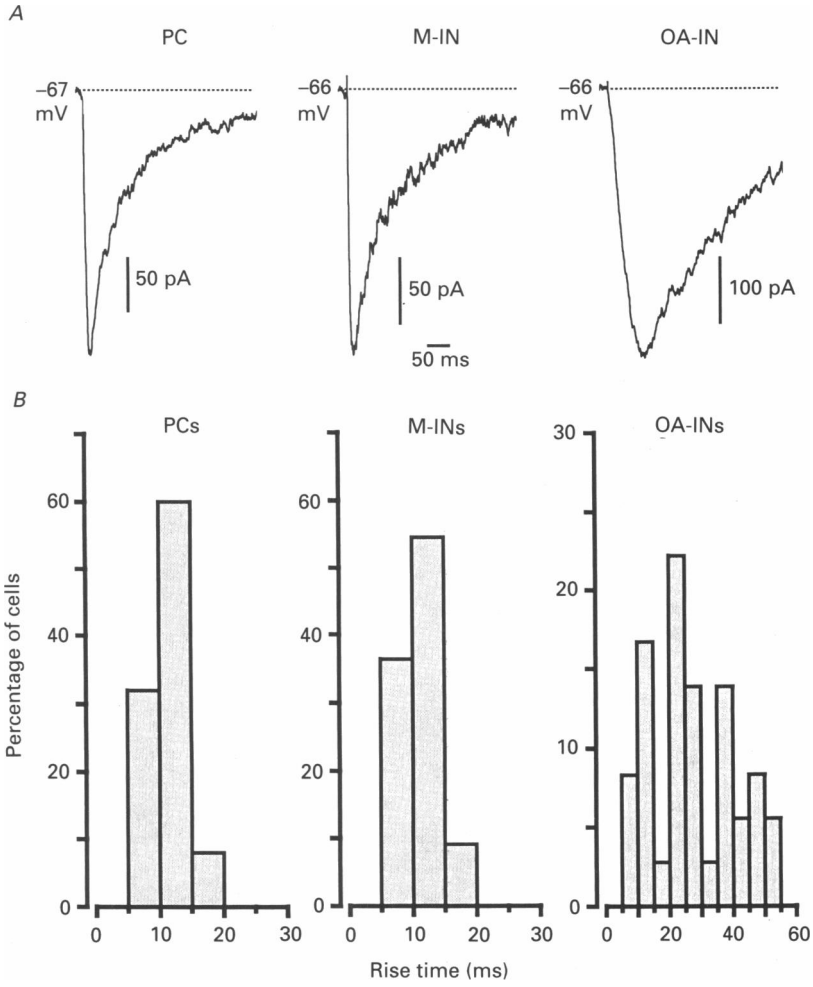

Fig. 4. Rise time of NMDA EPSCs in different CA1 neurones in 0 Mg^{2+} saline. *A*, representative NMDA EPSCs from a PC (left), a M-IN (middle) and an OA-IN (right) recorded at the indicated potentials. The PC and the M-IN had similar rise times (6·5 and 5 ms). The OA-IN, by contrast, showed a remarkably slow rise time (49 ms). Note that the current calibration for the OA-IN is double that for the other cells. Traces are averages of five consecutive records. *B*, distribution histograms of NMDA EPSC rise times in PCs (right), M-INs (middle) and OA-INs (right). The rise times are measured at holding potentials between −60 and −70 mV in 0 Mg^{2+} saline. Note the compressed time scale in the OA-IN histogram.

ranging from 4·5 to over 50 ms (mean 25·0±13·4 ms, $n = 37$; Fig. 4*B*). For further analysis, NMDA EPSCs in OA-INs were subdivided into two groups: *ordinary* NMDA EPSCs which had rise times up to 16 ms (mean 9·0±2·9, $n = 10$), and *slow*

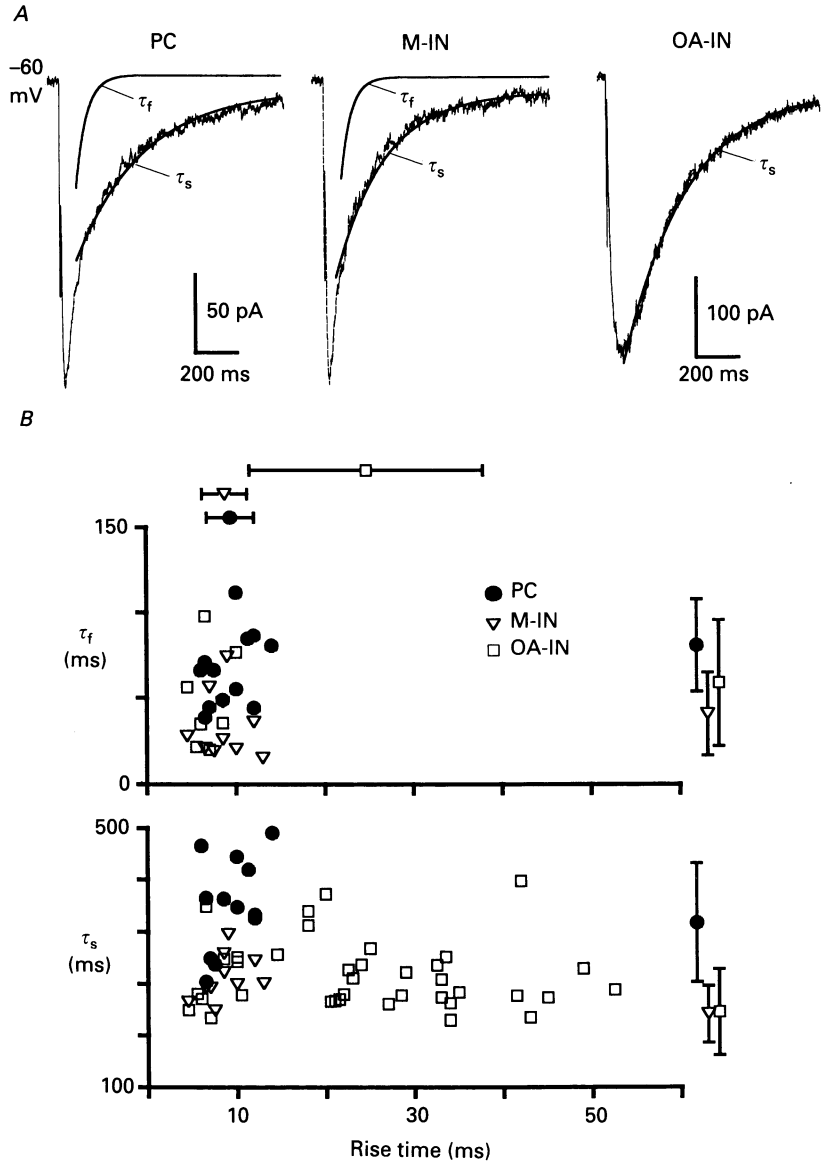

Fig. 5. Decay time course of NMDA EPSCs in different CA1 neurones in 0 Mg^{2+} saline. *A*, representative NMDA EPSCs from a PC (left), a M-IN (middle) and an OA-IN (right) recorded at the indicated potential. Each trace is an average of ten records. The decays of the EPSCs in PC and ML-IN were best fitted with two exponentials. The fast and slow decay components, designated τ_f and τ_s, are superimposed on the current traces. The decay of the EPSC in the OA-IN was best fitted with a single exponential. *B*, the time constants of NMDA EPSC decay, τ_f and τ_s, from twelve PCs (●), ten M-IN (▽) and thirty seven OA-INs (□) are plotted against their respective EPSC rise times. The mean ± S.D. rise times, and decay time constants are indicated above and on the right side of the figure, respectively. Note that in most OA-INs (30 out of 37), NMDA EPSCs decay with a single, slow time constant.

NMDA EPSCs whose rise times were above 16 ms (mean 31·2±10·35, $n = 26$). The slow NMDA EPSCs were significantly larger than ordinary currents in the three cell types. The average g_{max} of slow and ordinary NMDA EPSCs in OA-INs was 6·2–2·8 nS ($n = 8$) and 3·5±1·2 nS ($n = 4$), respectively.

Decay of NMDA EPSCs

Irrespective of cell type, the decay of NMDA EPSCs with ordinary rise time could be best fitted with a biexponential function in the vast majority of cells. By contrast, NMDA EPSCs with slow rise times decayed monoexponentially. Figure 5*A* compares ordinary NMDA EPSCs from a PC and a M-IN with a slow NMDA EPSC from an OA-IN. The currents in the PC and the M-IN had similar rise times (7 and 6 ms, respectively) and decayed biexponentially. The PC displayed longer fast (τ_f) and slow (τ_s) time constants of decay than the M-IN (38·3 and 246·1 ms *versus* 34·8 and 171·3 ms). The NMDA EPSC in the OA-IN, by contrast, had a rise time of 29 ms and decayed with a single time constant of 223 ms.

Part *B* of Fig. 5 summarizes the data from twelve PCs, ten M-INs and thirty seven OA-INs. The τ_f and τ_s from individual cells are plotted against the respective rise times of the currents. The mean rise times are indicated above the figure (PCs: 9·3±2·7; M-INs: 8·7±2·5; OA-INs: 24·8±13·0). The mean time constants are shown on the right side of the figure (M-INs: 34·4±19·3 and 212·4±44·0 ms, OA-INs: 48·3±26·1 and 215·8±66·6, for τ_f and τ_s respectively). Both time constants were longer in PCs (66·5±21·7 and 353·9±91·3 ms) than in INs.

The τ_s of NMDA EPSCs in M-INs (212·0±44·2 ms) was very similar to the τ_s or ordinary NMDA EPSCs in OA-INs (216·9±67·1 ms). These τ_ss were also identical to the single exponential decay time constants of slow NMDA EPSCs (217·2±69·1 ms), which therefore were plotted as τ_s in Fig. 5*B*.

The relative amplitudes of the fast (A_f) and slow (A_s) current components were −96·0±47·0 and −86·8±31·5 pA in PCs, −43·0±21·0 and −96·8±50·2 pA in M-INs, −76·3±57·2 and −137·2±66·7 pA in biexponentially decaying OA-INs (see Table 1). A_s was significantly larger in OA-INs than in PCs.

Effect of voltage

Changes in holding voltage had no systematic effect on rise time and decay of ordinary and slow NMDA EPSCs in all neurones investigated. In the slow NMDA EPSC illustrated in Fig. 6*A*, the rise time and decay time constant were, respectively, 22·5 and 171·0 ms at −75 mV, and 18·5 and 188·0 ms at 30 mV holding potential. The two traces were normalized and superimposed on the right side of the figure to illustrate the similarity of their time course. Part *B* shows the voltage dependence of rise times and decay time constants of NMDA EPSCs in ten OA-INs (rise times at −60 mV ranging from 10·5 to 52 ms). Both measured variables showed a small trend towards prolongation with depolarization. The differences, however, were not statistically significant.

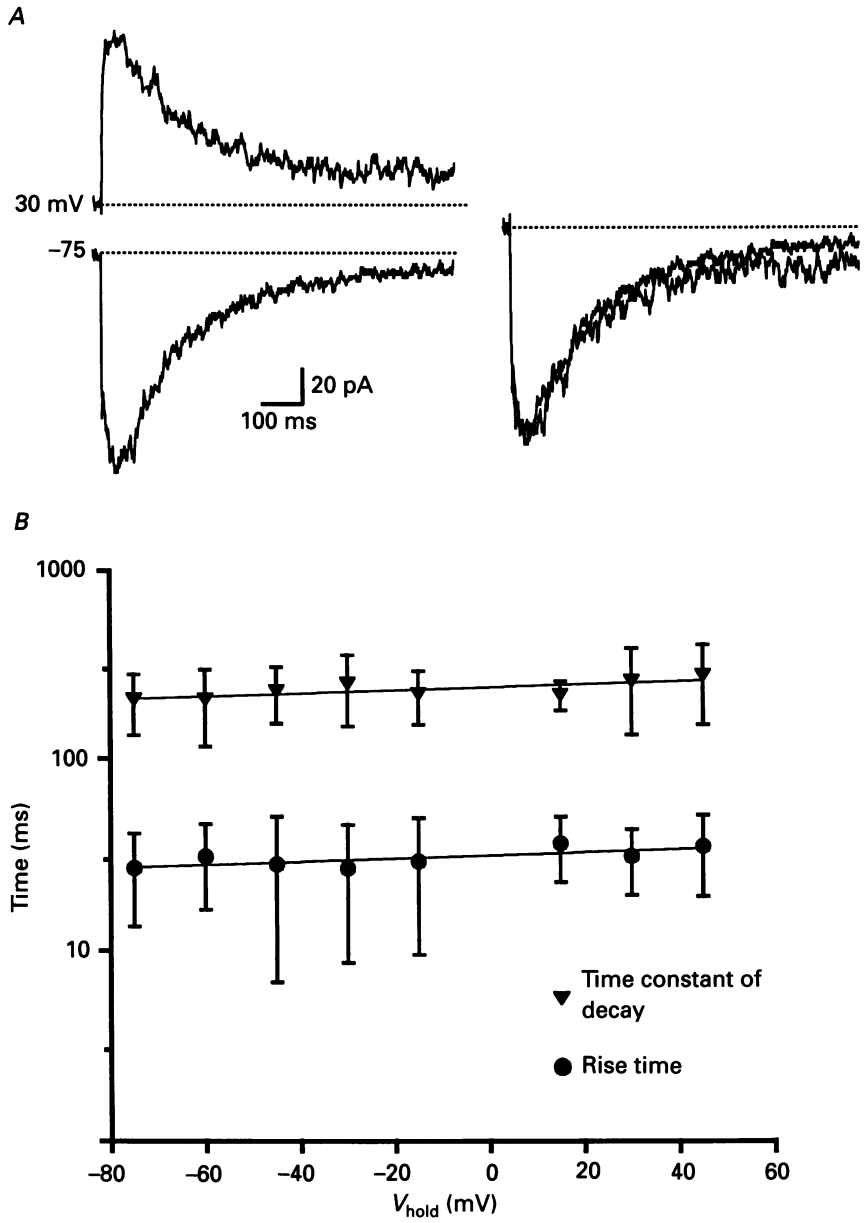

Fig. 6. Voltage insensitivity of NMDA EPSC time course in OA-INs. *A*, representative NMDA EPSCs from an OA-IN , recorded at two different voltages in nominally 0 Mg^{2+} saline. Rise time and decay were, respectively, 22·5 and 171 ms at −75 mV, and 18·5 and 188 ms at 30 mV. The two traces were superimposed on the right side. *B*, the rise times and time constants of decay of NMDA EPSCs recorded from ten OA-INs are plotted *versus* the holding voltage. No significant change in either rise time or decay upon depolarization was found.

Properties of slow NMDA EPSCs

Effect of stimulation location

When the stimulation electrode was moved around a M-IN, it was found that NMDA EPSCs could be evoked only from a few discrete locations. By contrast,

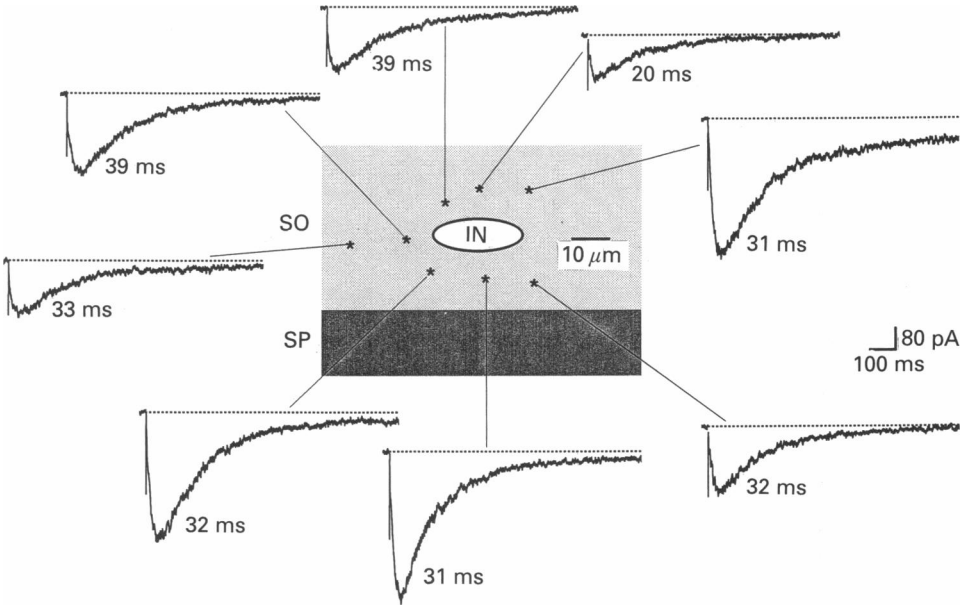

Fig. 7. Slow NMDA EPSCs evoked in an OA-IN by stimulating at different sites around the cell. The scheme depicts the stimulation sites, indicated by asterisks, in stratum oriens (SO). The cell body was oriented parallel to the pyramidal layer (SP). All EPSCs were evoked with the same stimulus intensity (85 μA). The rise times of the EPSCs are indicated. Note that in all cases the NMDA EPSC rise times were in the slow range.

NMDA EPSCs in OA-INs were usually evoked by stimulating anywhere around the cell. Figure 7 shows schematically the soma of an OA-IN oriented parallel to the PC layer (SP). NMDA EPSCs evoked by stimulating with the same intensity (85 μA) at the indicated places are illustrated with the corresponding rise times. It is evident that NMDA EPSCs evoked at all locations showed a prolonged rise time (ranging from 20 to 39 ms). This experiment was repeated in two other OA-INs with qualitatively similar results, suggesting that activation of NMDA EPSCs with slow rise times was not dependent on stimulation of a specific afferent pathway.

Effect of stimulation intensity

In adult hippocampal slices treated with $GABA_A$ receptor antagonists, supra-threshold stimulation of afferent pathways to CA1 neurones induces synchronized bursts (Schwartzkroin & Prince, 1978). Burst generation is all-or-none and requires recurrent excitatory synaptic transmission, which in Mg^{2+}-free saline containing

CNQX may be provided by NMDA receptor activation. Therefore, it is conceivable that the slow rise time of NMDA EPSCs was due to *polysynaptic* activation of OA-INs by synchronously bursting PCs.

To test this possibility we first examined how varying stimulation intensity affects the time course of slow NMDA EPSCs. The results of this experiment are illustrated

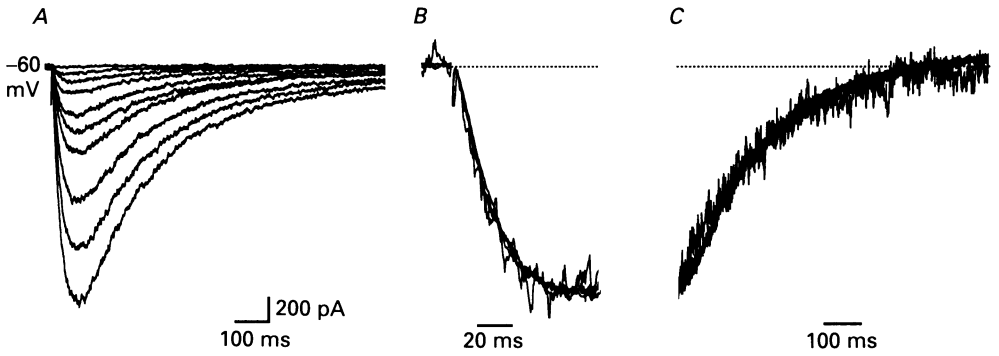

Fig. 8. Variation of stimulus intensity does not affect the kinetics of slow NMDA EPSCs. NMDA EPSCs were evoked from an OA-IN while increasing stimulus intensity from 50 to 120 μA. The peak EPSC amplitude increased gradually from −148 to −1800 pA (*A*). The traces in *B* and *C* are normalized portions of traces in *A*, depicting the rise times (*B*) and the decays (*C*) of NMDA EPSCs. The increase in EPSC amplitude was not accompanied by a prolongation of rise times.

in Fig. 8. Part *A* shows sample records of slow NMDA EPSCs from a OA-IN. With increasing stimulus intensity (50 to 120 μA), the amplitude of EPSCs increased from −148 to −1800 pA in a graded, rather than in an all-or-none, fashion. Parts *B* and *C* show the normalized rising and decaying sections of five EPSCs from *A*, evoked by different stimulus intensities. It can be seen that no systematic change in NMDA EPSC rise time occurred in this cell (rise time 39·7 ± 7·7 ms). Similar results were obtained from three additional OA-INs.

Effect of Mg^{2+}

Another way to test whether the slow NMDA EPSC rise time reflects NMDA receptor-mediated polysynaptic excitation of OA-INs was to suppress this activity by raising extracellular Mg^{2+}. Figure 9 shows slow NMDA EPSCs recorded at holding potentials of −60 and 15 mV in 0 (*A*) and in 1 mM (*B*) extracellular Mg^{2+}. Expectedly, most of the current at −60 mV was blocked by 1 mM Mg^{2+}. The reduction of the EPSC amplitude (from 86 to 65 pA) at 15 mV is most probably due to Mg^{2+} block of glutamate release. As seen in the normalized and superimposed traces in *C*, the rise time of NMDA EPSCs at 15 mV was slightly reduced by Mg^{2+} (from 26 ms in 0 Mg^{2+} to 20 ms in 1 mM Mg^{2+}). From seven OA-INs tested in this manner, only one showed reduction of rise time to the ordinary range (from 42 to 10 ms). In the six other cells the rise times slightly shortened upon adding Mg^{2+} (from 27·8 ± 8·3 ms to 22·3 ± 4·4 ms), but remained in the slow range. These findings argue against the possibility that the slow rise time of NMDA EPSCs is due to prolonged polysynaptic excitation.

Effects of low Ca^{2+} and of Cd^{2+}

Another possibility we considered for the origin of the slow NMDA EPSCs was the activation of endogenously bursting CA1 PCs (Masukawa, Benardo & Prince, 1982). These neurones generate a cluster of four or five action potentials lasting about 50 ms

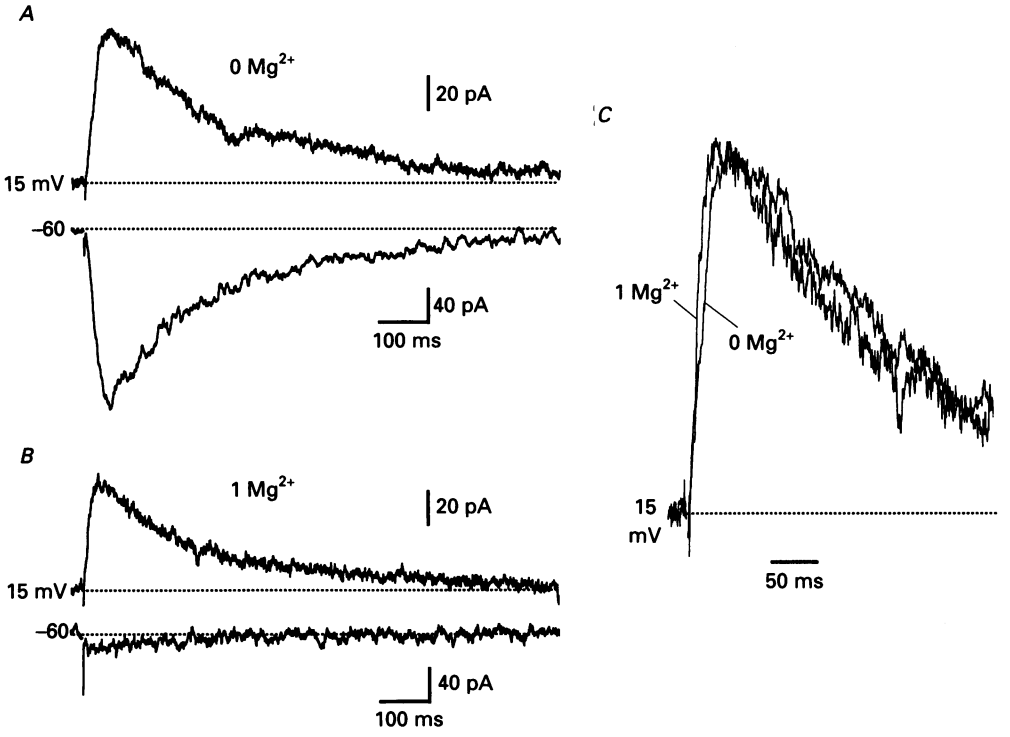

Fig. 9. Effect of increasing extracellular Mg^{2+} on slow NMDA EPSCs. NMDA EPSCs from an OA-IN were evoked at the indicated potentials in 0 Mg^{2+} saline (*A*) and after washing with 1 mM Mg^{2+} saline (*B*). The traces recorded at 15 mV were normalized and superimposed (*C*). Note that although the EPSC rise time shortened in 1 mM Mg^{2+} (from 26 to 20 ms), it remained in the slow range.

in response to afferent stimulation, provided that feed-forward and recurrent inhibition have been reduced by $GABA_A$ receptor blockers (Schwartzkroin & Prince, 1978). If this activity propagates through recurrent collaterals which synapse on OA-INs, then a repetitive *monosynaptic* excitation of the INs would be expected. To assess the contribution of this mechanism we perfused the slices with either nominally Ca^{2+}-free saline or with saline containing 25 μM Cd^{2+}. These treatments are expected to reduce endogenous bursting that is presumably mediated by Ca^{2+} currents in hippocampal PCs (Wong & Prince, 1978; Wong, Prince & Basbaum, 1979).

The results of both experiments are illustrated in Fig. 10. The NMDA EPSCs decreased continually as Ca^{2+} was being washed out (Fig. 10*A*), or as Cd^{2+} was

washed in (Fig. 10*B*). However, the rise time and decay of the currents did not change significantly. These findings suggest that the slow rise time of NMDA EPSCs in OA-IN was not a consequence of endogenously bursting presynaptic PCs.

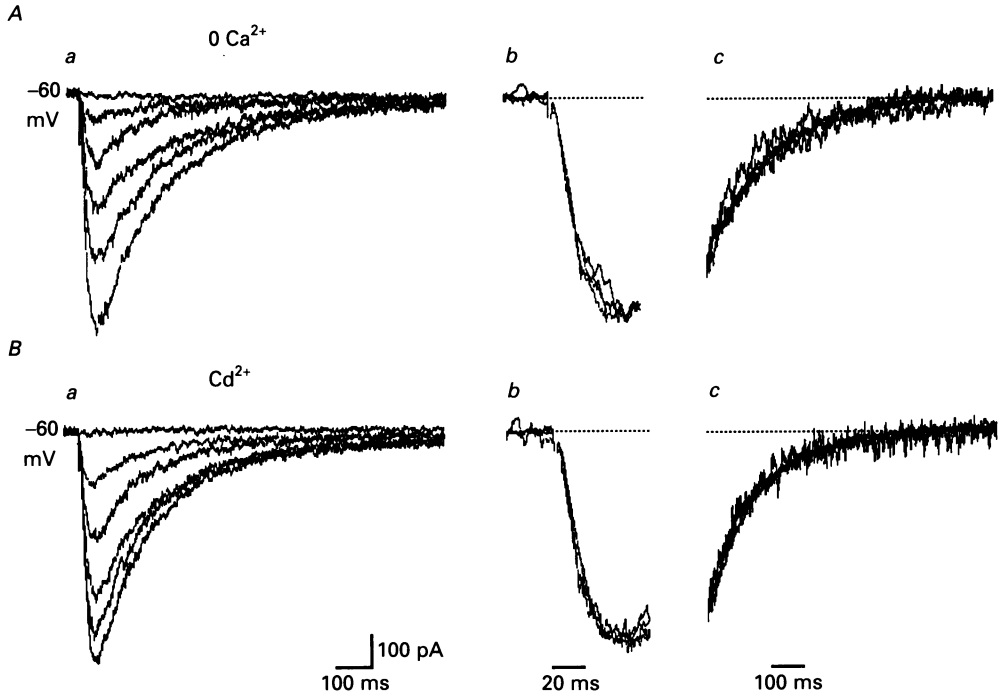

Fig. 10. Reduction of extracellular Ca^{2+} (*A*) or addition of Cd^{2+} (*B*) do not affect the kinetics of slow NMDA EPSCs. NMDA EPSCs were recorded from an OA-IN while the normal saline was exchanged for Ca^{2+}-free solution (*A*). After reintroduction of normal saline, 25 μM Cd^{2+} was added to the saline. The traces in *b* and *c* are normalized portions of traces in *a*, depicting the rise times (*b*) and the decay (*c*) of NMDA EPSCs. In both experiments EPSC amplitudes decreased to zero without a systematic change in either rise time or decay.

DISCUSSION

We have used the whole-cell recording mode of the patch-clamp technique to compare properties of pharmacologically isolated, agonist-induced and synaptic NMDA receptor-mediated currents in PCs and INs from different layers of the hippocampal CA1 area. With respect to the *I–V* relation and Mg^{2+} sensitivity, the agonist-induced currents and the NMDA EPSCs in PCs, M-INs and OA-INs were quite similar. However, we discovered significant differences and peculiarities in the kinetic properties of NMDA EPSCs in the three groups of neurones investigated.

I–V relation of NMDA receptor-mediated currents

In saline containing 1 or 2 mM Mg^{2+}, all *I–V* relations showed a region of negative slope conductance at voltages more negative than −20 to −30 mV. This region shifted to much more hyperpolarized potentials ($\leqslant -70$ mV) in nominally Mg^{2+}-free

saline, as expected from partial relief of the voltage-dependent block of NMDA receptor channels by Mg^{2+} (Nowak *et al.* 1984; Mayer *et al.* 1984).

The remaining non-linearity in the *I–V* relation at hyperpolarized potentials most probably reflects the presence of residual extracellular Mg^{2+}. We have attempted to estimate the residual [Mg^{2+}], by fitting the theoretical *I–V* function for the NMDA receptor-mediated conductance (eqn (7) in Methods) to the empirical *I–V* relations of NMDA EPSCs obtained in nominally Mg^{2+}-free saline. From the best fitted functions, the mean value of residual [Mg^{2+}] in nine slices was $14{\cdot}6 \pm 3{\cdot}4$ μM (PCs $13{\cdot}6 \pm 4{\cdot}1$ μM, $n = 5$; INs $15{\cdot}9 \pm 2{\cdot}0$ μM, $n = 4$; difference not significant). By contrast, the [Mg^{2+}] in our nominally Mg^{2+}-free saline, as measured with atomic absorption spectroscopy, was 2 μM. Therefore, residual [Mg^{2+}] cannot be accounted for by contamination in the saline. A more likely explanation is wash-out of intracellular Mg^{2+} into the extracellular compartment. Indeed, a marked decrease of intracellular [Mg^{2+}] (from 1·7 to 0·5 mM) during perfusion with Mg^{2+}-free solution, was demonstrated in frog skeletal muscle (Alvarez-Leefmans, Gamiño, Giraldez & Gonzalez-Serratos, 1986).

Kinetic properties of NMDA EPSCs

Analyses of the rise times and decays of NMDA EPSCs in the three classes of CA1 neurones in nominally 0 Mg^{2+} disclosed significant differences. Most notable was the finding of very slowly rising NMDA EPSCs in the majority of OA-INs. The mean rise time of NMDA EPSCs in these neurones (31·2 ms at a holding potential of -60 to -70 mV) was about three- to fourfold longer than in PCs, in M-INs and in the remaining OA-INs (Table 1). It was also much longer than the rise time of NMDA EPSCs recorded under similar conditions in rat dentate granule cells (6·4 ms, Keller *et al.* 1991). The possible mechanisms of this peculiar feature are discussed below.

Irrespective of cell type, NMDA EPSCs with ordinary rise times (i.e. between 4·5 and 16 ms) displayed a slow, biexponential decay. However, the decay of NMDA EPSCs was considerably and significantly faster in INs than in PCs (Table 1). INs differed from PCs also in the relative contribution of the two components to the peak current. The fast component progressively contributed less in the order PCs > OA-INs with ordinary NMDA EPSCs > M-INs > OA-INs with slow NMDA EPSCs. It is unlikely that these differences are due to a different localization of excitatory synapses on OA-INs, since the rise times of non-NMDA EPSCs in all three cell types were found to be the same (M. Perouansky & Y. Yaari, unpublished observations). Interestingly, NMDA EPSCs in dentate granule cells also decayed biexponentially with a time course remarkably similar to that of NMDA EPSCs in PCs (Table 1), with similar relative contribution of A_f and A_s to the peak amplitude (Konnerth *et al.* 1990; Keller *et al.* 1991). In contrast to the findings in dentate granule cells, however, and in agreement with results obtained from adult CA1 PCs (Hestrin *et al.* 1990*a*), the time constants of decay were not consistently prolonged by depolarization in the studied cell types.

Recent studies in thin hippocampal slices (Hestrin *et al.* 1990*b*; Konnerth *et al.* 1990) and in cultures of synaptically connected hippocampal neurones (Lester, Clements, Westbrook & Jahr, 1990), suggest that the time course of ordinary NMDA EPSCs is determined primarily by slow kinetics of the NMDA receptor channel,

rather than by prolonged action of the transmitter (due to slow diffusion or uptake). Since the open time of single NMDA receptor channels is within the range of 5–15 ms (Cull-Candy & Usowicz, 1987; Jahr & Stevens, 1987; Ascher, Bregestowski & Nowak, 1988), the mean open time cannot be the 'elementary event' that determines the decay of NMDA EPSCs. However, the activity of NMDA receptor channels in

TABLE 1. Summary of kinetic characteristics of NMDA EPSCs in different hippocampal neurones

	PCs	M-INs	OA-INs ordinary	OA-INs slow	Granule cells
Rise times (ms)	9·3 ± 2·7	9·1 ± 3·2	7·3 ± 1·8	31·20 ± 10·35	6·4
τ_f (ms)	66·5 ± 21·7	34·4 ± 19·3	48·3 ± 26·1	—	84
τ_s (ms)	353·9 ± 91·3	212·5 ± 44·2	212·0 ± 75·6	217·2 ± 69·1	330
A_f (pA)	−96·8 ± 47·0	−43·0 ± 21·0	−76·3 ± 57·2	—	−95
A_s (pA)	−86·8 ± 31·5	−96·8 ± 50·2	−137·2 ± 66·7	−349 ± 220	−95
A_f/A_s	1·12	0·44	0·56	—	1
n	12	10	7	28	4

τ_f and τ_s are the fast and slow time constants of decay, A_f and A_s the corresponding relative current amplitudes of the two components. The data for NMDA EPSCs in CA1 PCs, M-INs and OA-INs are the results of this study. The parameters are given for the same set of cells in each column. The NMDA EPSCs in OA-INs were subdivided into two subgroups according to the rise time (ordinary *versus* slow). Data for NMDA EPSCs in granule cells are taken from Keller *et al.* 1991. The rise time of NMDA EPSCs in slow OA-INs was significantly slower than in all other cell types studied. τ_s was significantly slower in PCs than in all types of INs, τ_f was significantly slower in PCs than in M-INs. A_s was significantly bigger in OA-INs than in PCs.

outside-out patches tends to appear in clusters lasting hundreds of milliseconds (Jahr & Stevens, 1987; Howe, Colquhoun & Cull-Candy, 1988; Keller *et al.* 1991) even after pulse-like applications of agonist (Lester *et al.* 1990). Thus, cluster kinetics most probably determines the decay of NMDA EPSCs. It is tempting to speculate that differences in NMDA receptor subunits expressed in hippocampal PCs and INs underlie the different time courses of NMDA EPSCs. Whether these differences are related to the differential localization of excitatory synapses on dendritic spines in PCs and on dendritic shafts in INs (Seress & Ribak, 1985) remains to be clarified. In this respect, the similarity of the decay of NMDA EPSCs in PCs and dentate granule cells (Table 1), which also bear spines on their dendrites (Ribak, Seress & Amaral, 1985), raises the possibility of spine filtering. Interestingly, it was recently found in the rat hippocampal hilus, that non-NMDA EPSCs are significantly slower in spiny *versus* aspiny neurones (Livsey & Vicino, 1992). However, current kinetics are not expected to change according to some spine models (Koch & Poggio, 1983).

Whatever the mechanism, our findings indicate a basic difference between NMDA EPSCs in principal neurones (PCs and granule cells) *versus* INs that may have functional consequences for neurotransmission and synaptic plasticity.

Unusual NMDA EPSCs in OA-INs

The rise time scatter of NMDA EPSCs in OA-INs was much wider than in PCs and M-INs, ranging from 4·5 to over 50 ms. We identified two subgroups within the OA-INs. One had NMDA EPSC rise times in the ordinary range, i.e. 4·5–16 ms. The

NMDA EPSCs in most of these INs decayed biexponentially, and were thus similar to the currents recorded from M-INs. The other group included INs with slow NMDA EPSC rise times ranging from 18 to over 50 ms. These currents decayed monoexponentially with a time constant similar to the τ_s of ordinary NMDA EPSCs. They were also much larger than all other NMDA EPSCs (Table 1) and readily evoked by stimulating anywhere around the cell.

Mechanism of the slow NMDA EPSC

Several mechanisms may possibly cause the unusually slow NMDA EPSC. In contrast to M-INs, OA-INs receive excitatory input not only from the Schaffer collateral–commissural system, but also from axon collaterals of CA1 PCs (Lacaille *et al.* 1987). Activation of CA1 PCs in conventional hippocampal slices (i.e. about 0·5 mm thick slices from adult animals) treated with $GABA_A$ receptor blockers, causes recurrent excitation that culminates in a synchronized burst that lasts 50–100 ms (Schwartzkroin & Prince, 1978; Hablitz, 1984). Furthermore, a subclass of CA1 PCs possesses endogenous burst characteristics and fires repetitively even upon brief stimulation (Masukawa *et al.* 1982). Burst activity propagating through recurrent collaterals of CA1 PCs would be expected to produce slowly rising EPSCs in target neurones. It should be noted, however, that the experimental conditions we employed (e.g. thin slices that limit recurrent synaptic connections, CNQX that blocks non-NMDA receptor-mediated synaptic excitation, room temperature and low extracellular K^+ concentration) did not favour the development of synchronous or endogenous bursting. Indeed, in current-clamp recordings from six CA1 PCs we did not detect the presence of endogenous bursters.

Several lines of evidence confirmed that the slow NMDA EPSCs are not underlain by repetitive polysynaptic or monosynaptic excitation of OA-INs. Firstly, the slow NMDA EPSCs increased gradually with stimulation intensity, rather than displaying the all-or-none behaviour of synchronous bursts. Secondly, the rise time of slow NMDA EPSCs at positive membrane voltage was not converted into the ordinary range by blocking NMDA receptor-mediated polysynaptic transmission with extracellular Mg^{2+}. Thirdly, reducing extracellular Ca^{2+} or adding Cd^{2+}, treatments expected to attenuate polysynaptic transmission and endogenous bursting, also did not affect the rise time of slow NMDA EPSCs. Finally, the rise time of the non-NMDA EPSC component (recorded in the absence of CNQX) in OA-INs with slow NMDA EPSCs, did not differ from that recorded from the other cell types (M. Perouansky & Y. Yaari, unpublished observations).

An alternative mechanism for the slow NMDA EPSCs could be diffusion of released glutamate to neighbouring synaptic or extrasynaptic NMDA receptors, assuming either comparatively higher density of these receptors on OA-INs and/or less efficient uptake of glutamate into the surrounding neuropil. Both conditions could explain the larger agonist-induced conductance increase in OA-INs ($22·9 \pm 5·4$ nS) compared to M-INs ($12·2 \pm 2·7$ nS). The spill-over of transmitter to neighbouring receptors could account for the significantly larger average peak currents observed in slowly rising NMDA EPSCs *versus* NMDA EPSCs in PCs and M-INs (Table 1). It could also mask τ_f, accounting for the apparently monoexponential decay of slow NMDA EPSCs.

It should be noted, however, that NMDA receptors in cultured cerebral neurones are concentrated at discrete synapses, the density of extrasynaptic receptors being less than 5% of the density at synapses (Jones & Baughman, 1991). Thus, even with reduced uptake of transmitter, the contribution of extrasynaptic NMDA receptors to the overall current is likely to be minor.

Finally, the unusually slow rise time of NMDA EPSCs may reflect exceptionally slow activation kinetics of NMDA receptor channels in OA-INs. Our data to date do not allow us to exclude either transmitter spill-over or the slow activation kinetic hypothesis for the generation of slow NMDA EPSCs.

We thank Dr A. Konnerth for his help in implementing the thin slice technique in our laboratory. We are also grateful to Drs S. Ginsbourg and M. S. Jensen for helpful discussions and Mr M. Pinco for help with the statistical analysis. This work was supported by the German–Israeli Foundation for Scientific Research and Development (GIF) and by a fellowship to M.P. from the MINERVA-Foundation.

REFERENCES

ALVAREZ-LEEFMANS, F. J., GAMIÑO, S. M., GIRALDEZ, F. & GONZALEZ-SERRATOS, H. (1986). Intracellular free magnesium in frog skeletal muscle fibres measured with ion-selective microelectrodes. *Journal of Physiology* **378**, 461–483.

ANDREASEN, M., LAMBERT, J. D. C. & JENSEN, M. S. (1989). Effects of non-*N*-methyl-D-aspartate antagonists on synaptic transmission in the *in vitro* hippocampus. *Journal of Physiology* **414**, 317–336.

ASCHER, P., BREGESTOSKI, P. & NOWAK, L. (1988). *N*-methyl-D-aspartate-activated channels of mouse central neurones in magnesium-free solutions. *Journal of Physiology* **399**, 207–226.

ASCHER, P. & NOWAK, L. (1988). The role of divalent cations in the *N*-methyl-D-aspartate responses of mouse central neurones in culture. *Journal of Physiology* **399**, 247–266.

BIRCH, P. J., GROSSMANN, C. J. & HAYES, A. G. (1988). 6,7-Dinitro-quinoxaline-2,3-dione and 6-nitro, 7-cyanoquinoxaline-2,3-dion antagonise responses to NMDA in the rat spinal cord via an action at the strychnine-insensitive glycine receptor. *European Journal of Pharmacology* **156**, 177–180.

BLAKE, J. F., BROWN, M. W. & COLLINGRIDGE, G. L. (1988). CNQX blocks acidic amino acid induced depolarizations and synaptic components mediated by non-NMDA receptors in rat hippocampal slices. *Neuroscience Letters* **89**, 182–186.

COLLINGRIDGE, G. L., HERRON, C. E. & LESTER, R. A. J. (1988). Synaptic activation of *N*-methyl-D-aspartate receptors in the Schaffer collateral–commissural pathway of rat hippocampus. *Journal of Physiology* **399**, 283–300.

CONNORS, B. W. & PRINCE, D. A. (1982). Effects of local anesthetic QX314 on the membrane properties of hippocampal pyramidal cells. *Journal of Pharmacology and Experimental Therapeutics* **220**, 476–481.

CULL-CANDY, S. G. & USOWICZ, M. M. (1987). Multiple-conductance channels activated by excitatory amino acids in cerebellar neurones. *Nature* **325**, 525–528.

EDWARDS, F. A., KONNERTH, A., SAKMANN, B. & TAKAHASHI, T. (1989). A thin slice preparation for patch clamp recordings from synaptically connected neurones of the mammalian central nervous system. *Pflügers Archiv* **414**, 600–612.

FRAZIER, D. T., NARAHASHI, T. & YAMADA, M. (1970). The site of action and active form of local anaesthetics. II. Experiments with quarternary compounds. *Journal of Pharmacology and Experimental Therapeutics* **171**, 45–51.

HABLITZ, J. J. (1984). Picrotoxin-induced epileptiform activity in hippocampus: role of endogenous versus synaptic factors. *Journal of Neurophysiology* **51**, 1011–1027.

HARRIS, E. W., GANONG, A. H. & COTMAN, C. W. (1984). Long-term potentiation in the hippocampus involves activation of *N*-methyl-D-aspartate receptors. *Brain Research* **323**, 132–137.

HESTRIN, S., NICOLL, R. A., PERKEL, D. J. & SAH, P. (1990*a*). Analysis of excitatory synaptic action in pyramidal cells using whole-cell recording from rat hippocampal slices. *Journal of Physiology* **422**, 203–225.

HESTRIN, S., SAH, P. & NICOLL, R. A. (1990*b*). Mechanism generating the time course of dual component excitatory synaptic currents recorded in hippocampal slices. *Neuron* **5**, 247–253.

HONORE, T., DAVIES, S. N., DREJER, J., FLETCHER, E. J., JACOBSEN, P., LODGE, D. & NIELSEN, F. E. (1988). Quinoxalinediones: potent competitive non-NMDA glutamate receptor antagonists. *Science* **241**, 701–703.

HOWE, J. R., COLQUHOUN, D. & CULL-CANDY, S. G. (1988). On the kinetics of large-conductance glutamate receptor ion channels in rat cerebellar granule neurones. *Proceedings of the Royal Society* B**233**, 407–422.

JAHR, C. E. & STEVENS, C. F. (1987). Glutamate activates multiple single channel conductances in hippocampal neurones. *Nature* **325**, 522–525.

JONES, K. A. & BAUGHMAN, R. W. (1991). Both NMDA and non-NMDA subtypes of glutamate receptors are concentrated at synapses on cerebral cortical neurons in culture. *Neuron* **7**, 593–603.

KAY, A. R., MILES, R. & WONG, R. K. S. (1986). Intracellular fluoride alters the kinetic properties of calcium currents facilitating the investigation of synaptic events in hippocampal neurons. *Journal of Neuroscience* **6**, 2915–2920.

KELLER, B. U., KONNERTH, A. & YAARI, Y. (1991). Patch clamp analysis of excitatory synaptic currents in granule cells of rat hippocampus. *Journal of Physiology* **435**, 275–293.

KOCH, C. & POGGIO, T. (1983). A theoretical analysis of electrical properties of spines. *Proceedings of the Royal Society* B**218**, 455–477.

KONNERTH, A., KELLER, B. U., BALLANYI, K. & YAARI, Y. (1990). Voltage sensitivity of NMDA-receptor-mediated postsynaptic currents. *Experimental Brain Research* **81**, 209–212.

KOSTYUK, P. G., KRISHTAL, O. A. & PIDOPLICHKO, V. I. (1975). Effects of internal fluoride and phosphate on membrane currents during intracellular dialysis of nerve cells. *Nature* **257**, 691–693.

LACAILLE, J. C., MULLER, A. L., KUNKEL, D. D. & SCHWARTZKROIN, P. A. (1987). Local circuit interactions between oriens/alveus interneurons and CA1 pyramidal cells in hippocampal slices: electrophysiology and morphology. *Journal of Neuroscience* **7**, 1979–1983.

LACAILLE, J. C. & SCHWARTZKROIN, P. A. (1988). Stratum lacunosum-moleculaire interneurons of hippocampal CA1 region. I. Intracellular response characteristics, synaptic responses, and morphology. *Journal of Neuroscience* **8** (4), 1400–1410.

LESTER, A. J., CLEMENTS, J. D., WESTBROOK, G. L. & JAHR, C. E. (1990). Channel kinetics determine the time course of NMDA receptor-mediated synaptic currents. *Nature* **346**, 565–567.

LIVSEY, C. T. & VICINO, S. (1992). Slower spontaneous excitatory postsynaptic currents in spiny versus aspiny hilar neurons. *Neuron* **8**, 745–755.

LORENTE DE NÓ, R. (1934). Studies on the structure of the cerebral cortex, II. Continuation of the study of the ammonic system. *Journal of Psychology and Neurology* **46**, 113–177.

MACDERMOTT, A. B., MAYER, M. L., WESTBROOK, G. L., SMITH, S. S. & BARKER, J. L. (1986). NMDA-receptor activation increases cytoplasmic calcium concentration in cultured spinal cord neurones. *Nature* **321**, 519–522.

MCNAMARA, J. O., RUSSELL, T. D., RIGSBEE, L. & BONHAUS, D. W. (1988). Anticonvulsant and antiepileptogenic actions of MK-801 in the kindling and electroshock models. *Neuropharmacology* **27**, 563–568.

MADISON, D. V. & NICOLL, R. A. (1984). Control of the repetitive discharge of rat CA1 pyramidal neurons *in vitro*. *Journal of Physiology* **354**, 319–331.

MASUKAWA, L. M., BENARDO, L. S. & PRINCE, D. A. (1982). Variations in electrophysiological properties of hippocampal neurons in different subfields. *Brain Research* **242**, 341–344.

MAYER, M., WESTBROOK, G. L. & GUTHRIE, P. B. (1984). Voltage-dependent block by Mg^{2+} of NMDA responses in spinal cord neurons. *Nature* **309**, 261–263.

MODY, I., STANTON, P. K. & HEINEMANN, U. (1988). Activation of *N*-methyl-D-aspartate receptors parallels changes in cellular and synaptic properties of dentate gyrus granule cells after kindling. *Journal of Neurophysiology* **59**, 1033–1054.

MONAGHAN, D. T. & COTMAN, C. W. (1985). Distribution of *N*-methyl-D-aspartate-sensitive L-[^{3}H] glutamate-binding sites in rat brain. *Journal of Neuroscience* **6**, 2909–2919.

NOWAK, L., BREGESTOWSKI, P., ASCHER, P., HERBET, A. & PROCHIANTZ, A. (1984). Magnesium gates glutamate-activated channels in mouse central neurones. *Nature* **307**, 462–465.

RIBAK, C. E., SERESS, L. & AMARAL, D. G. (1985). The development, ultrastructure and connections of the mossy cells of the dentate gyrus. *Journal of Neurocytology* **14**, 835–857.

SAH, P., HESTRIN, S. & NICOLL, R. A. (1990). Properties of excitatory postsynaptic currents recorded *in vitro* from rat hippocampal interneurones. *Journal of Physiology* **430**, 605–616.

SCHWARTZKROIN, P. A. & PRINCE, D. A. (1978). Cellular and field potential properties of epileptogenic hippocampal slices. *Brain Research* **147**, 117–130.

SERESS, L. & RIBAK, C. E. (1985). A combined Golgi–electron microscopic study of non-pyramidal neurons in the CA1 area of the hippocampus. *Journal of Neurocytology* **14**, 717–730.

SMART,. T. G. (1989). Excitatory amino acids: the involvement of second messengers in the signal transduction process. *Cellular and Molecular Neurobiology* **9**, 193–206.

THOMSON, A. M., WALKER, V. E. & FLYNN, D. M. (1989). Glycine enhances NMDA receptor-mediated synaptic potentials in neocortical slices. *Nature* **338**, 422–424.

WONG, R. K. S. & PRINCE, D. A. (1978). Participation of calcium spikes during intrinsic burst firing in hippocampal neurons. *Brain Research* **159**, 385–390.

WONG, R. K. S., PRINCE, D. A. & BASBAUM, A. I. (1979). Intradendritic recordings from hippocampal neurons. *Proceedings of the National Academy of Sciences of the USA* **76**, 986–990.